

Coherent Receiver for L-band

Misaki GOTOH*, Kenji SAKURAI, Munetaka KUROKAWA, Ken ASHIZAWA, Yoshihiro YONEDA, and Yasushi FUJIMURA

As a solution to the rapidly increasing optical traffic, 100 Gbit/s transmission systems using the digital coherent optical communication technology has been adopted in high-speed and large-capacity optical transmission. Optical transceivers are required to be operable in the long wavelength band (L-band) in addition to the conventional band (C-band). Based on the design of C-band receivers, we have developed compact optical receivers for the L-band operation. This paper presents the design and typical characteristics of the new optical receivers.

Keywords: L-band, coherent receiver, 90° hybrid

1. Introduction

Recently, the demand for diverse networks has been increasing rapidly due to the widespread use of the Internet of Things (IoT) technology in various fields, high-definition video distribution services, and new cloud computing applications. To meet the demand, large-capacity transmission systems that use digital coherent optical communication technologies, such as Dual-Polarization Quadrature Phase Shift Keying (DP-QPSK)*¹ and have transmission speed exceeding 100 Gbit/s have been widely deployed for metro networks and long haul networks around the world. The data traffic on these networks is expected to increase in speed and volume, and therefore multiplexing using the L-band (in addition to the conventional C-band) will be necessary to increase the symbol rate and enhance multi-level encoding. Notably, the transmission capacity can be doubled by expansion to the L-band where two bands are used in parallel on existing fiber optics, enabling the transmission capacity to be increased more easily compared to other means.

We previously developed a compact coherent receiver (Micro-ICR)⁽¹⁾ as an optical receiver that can be installed in CFP2 optical transceivers for the C-band, and obtained satisfactory characteristics.

We have developed a compact coherent receiver with high responsivity characteristics for the L-band. This paper reports on the results.

2. Configuration of the Coherent Receiver

2-1 Configuration of the coherent receiver module

Photo 1 shows the appearance of the coherent receiver, and Fig. 1 shows the configuration diagram.

The package size is 12.0 × 22.7 × 4.5 mm. As in the case of the Micro-ICR for the C-band, the coherent receiver conforms to the Micro-ICR Type 1 standard⁽²⁾ of the Optical Internetworking Forum (OIF),*² and can be installed in CFP2 optical transceivers. Receivers for digital coherent optical communication are designed to separate phase-modulated, polarization-multiplexed signal light into a horizontally polarized wave (Y-polarization) and vertically polarized wave (X-polarization), which then interfere

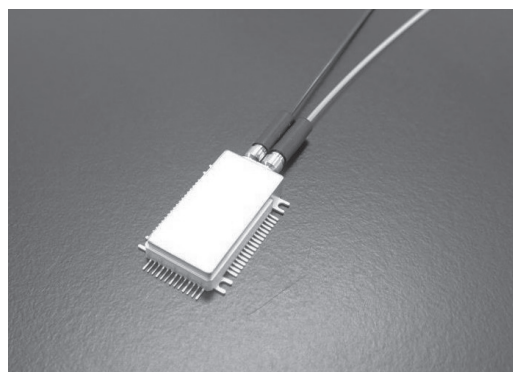


Photo 1. Appearance of the coherent receiver

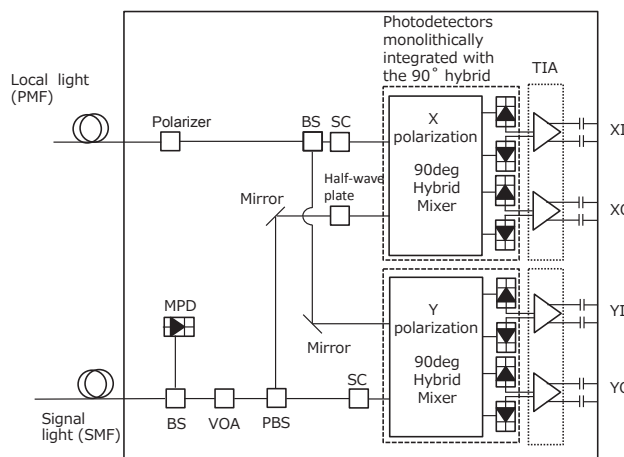


Fig. 1. Configuration diagram

with the local light to detect the in-phase (I) and quadrature (Q) components of each polarization to achieve conversion into four pairs of high-speed differential electric signals (XI/XQ/YI/YQ). Each component must be separated accurately, and the amplitude and phase between separated signals must be maintained stably to convert light to electricity.

This device was designed using our high-integration and high-density implementation technologies as for the Micro-ICR for the C-band.

An incident signal light passes through the beam splitter (BS) for the power monitor PD (MPD) and the variable optical attenuator (VOA). The X- and Y- polarized waves are then separated by the polarizing beam splitter (PBS).

The Y-polarized wave passes through the skew correction device (SC) that compensates for the optical path difference between the two polarized waves, and is concentrated into the input waveguide of the 90° hybrid integrated photodetector.

Meanwhile, the X-polarized wave is reflected by a mirror, passes through the half-wave plate that aligns the polarization direction, and is concentrated into the input waveguide of another 90° hybrid integrated photodetector.

The local light passes through the polarizer that aligns the polarization direction, is separated by the BS into two optical paths, and is concentrated into the input waveguide of respective 90° hybrid integrated photodetectors. The signal light interferes with the local light in the 90° hybrid integrated photodetectors, and is separated into respective components and then converted from light into current with the balanced photodiode (PD), which multiplexes the two PD outputs.

Subsequently, the current is subject to voltage conversion and amplification with the transimpedance amplifier (TIA) and is output from the high-frequency terminal.

The basic configuration is the same as that of the coherent receiver for the C-band. To receive the L-band, the transmission and reflection characteristics of the 90° hybrid integrated photodetectors and optical parts were optimized for the L-band.

2-2 Photodetectors monolithically integrated with the 90° hybrid

The 90° hybrid integrated photodetectors, which were developed using our proprietary InP-based photonic integrated technology, are the key devices that determine the characteristics of a coherent receiver.

The top view of the 90° hybrid integrated photodetector is shown in Fig. 2 (a), and the block diagram is shown in Fig. 2 (b). The 90° hybrid and four waveguide type pin-PDs are integrated as a single chip on an InP substrate.

The 90° hybrid section is comprised of the 2×4 MMI³ working as a 180° hybrid for in-phase relation, the 45° phase shifter, and the 2×2 MMI working for quadrature phase relation. This structure makes it possible to avoid crossing the output waveguides and to connect to the PD of each channel, thereby eliminating optical loss and crosstalk.⁽³⁾

In the waveguide type pin-PD section, the core layer (i-GaInAsP) of the 90° hybrid output waveguide is butt-jointed with the optical absorption layer (i-GaInAs) of the PD. This structure is advantageous for achieving high responsivity.⁽³⁾

The responsivity characteristics of the 90° hybrid integrated photodetector are determined by the product of the transmittance of the 90° hybrid and the responsivity of the PD section. These factors need to be optimized for photo-

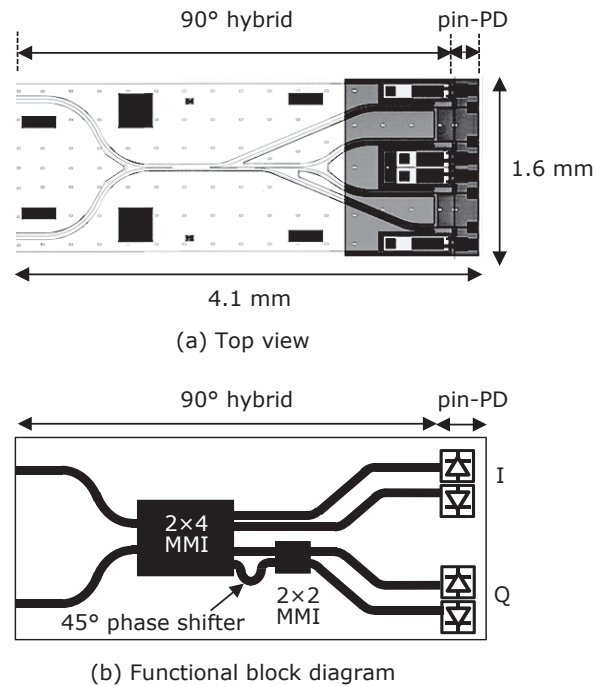


Fig. 2. Photodetectors monolithically integrated with the 90° hybrid

detection over the L-band wavelength range.

Regarding the 90° hybrid section, the dimensions of the two MMIs and the 45° phase shifter were optimized to maximize the transmittance at the center of the wavelength range. The center wavelength of the C-band was set to 1550 nm, while that of the L-band was set to 1587 nm.

The normalized transmittance spectra of the fabricated 90° hybrid are shown in Fig. 3. The transmittance at the center wavelength of the L-band was comparable to that of the C-band.

Regarding the waveguide type pin-PD section, the optical signal in the L-band is photodetected at the wavelength range close to the absorption end of GaInAs. Therefore, under low temperature, the sudden drop of responsivity may be caused because the absorption coefficient of GaInAs changes significantly with a temperature variation. To compensate for a decrease in the absorption

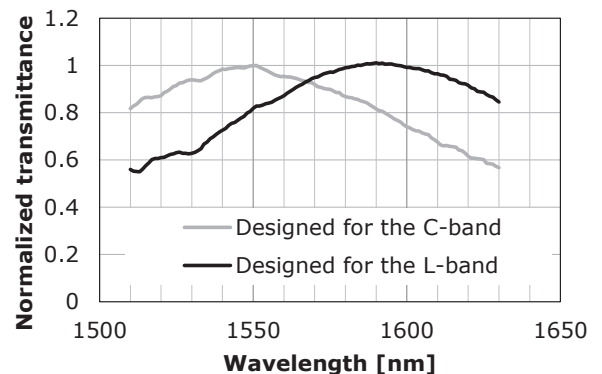


Fig. 3. Normalized transmittance spectra of the 90° hybrid

coefficient in a low-temperature environment, the PD was optimized by making it long in the waveguide direction (in terms of the length of the absorption layer in the propagation direction of light).

We fabricated an independent element that incorporated only the pin-PD section (i.e., without the 90° hybrid section). Figure 4 shows the temperature characteristics (at -5, 25, and 85°C) of responsivity (normalized at 25°C and wavelength of 1615 nm) from the C-band up to the L-band. We confirmed that the decrease in responsivity under low temperature was suppressed in the L-band.⁽⁴⁾

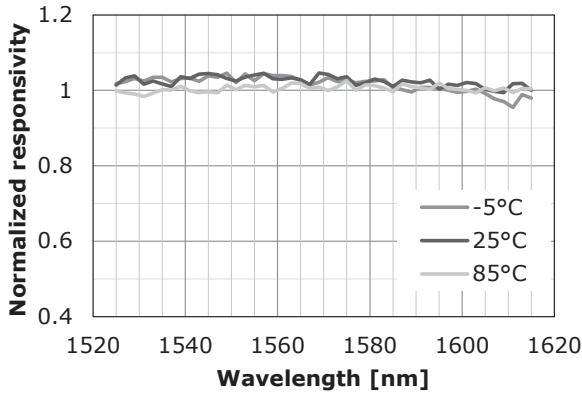


Fig. 4. Normalized responsivity of the waveguide type pin-PD without the 90° hybrid

3. Development Target Specifications

Table 1 shows the development target specifications of the L-band coherent receiver. To enable expansion from the C-band to the L-band based on the OIF’s Micro-ICR Class 20 standard, we aimed to achieve equivalent characteristics (except for the band) to those of our coherent receiver for the C-band.

Table 1. Development target characteristics

Item	Condition	Min.	Max.	Unit
Operating temperature		-5	85	°C
Operating frequency	L-band	186.0	191.5	THz
Operating wavelength		1565.50	1611.79	nm
Responsivity	Local light	0.05	0.1	A/W
	Signal light	0.05	0.1	
Polarization extinction ratio		20		dB
Phase Error		-7.5	7.5	deg
Bandwidth	-3dB	20		GHz
Common-mode rejection ratio (CMRR)	Signal light	DC	-20	dB
		~20GHz	-16	
	Local light	DC	-16	
		~20GHz	-14	

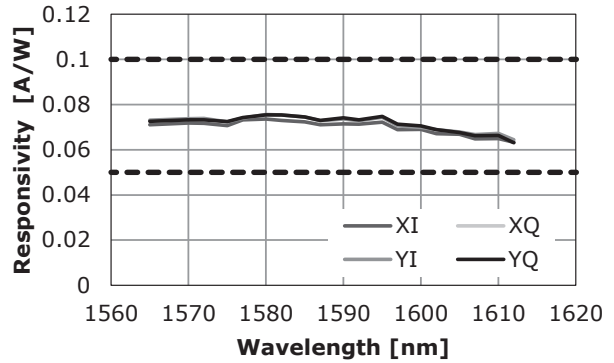
4. Characteristics of the Coherent Receiver

4-1 Responsivity characteristics

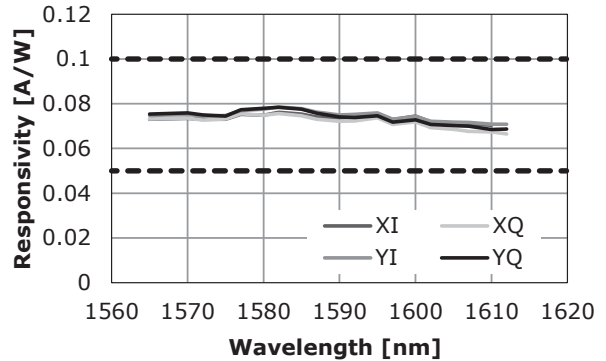
The coherent receiver’s wavelength dependence of signal light responsivity in the L-band is shown in Fig. 5 (a), and the wavelength dependence of local light responsivity is shown in Fig. 5 (b).

Responsivity of more than 0.06 A/W was attained within the operating wavelength range for both the signal light and local light, achieving the target characteristics. The characteristics are considered to be highly favorable with minimal deviation between the channels.

Responsivity characteristics were equivalent to those of our coherent receiver for the C-band, indicating that the 90° hybrid integrated photodetector optimized for the L-band was fabricated as designed.



(a) Signal light (25°C)



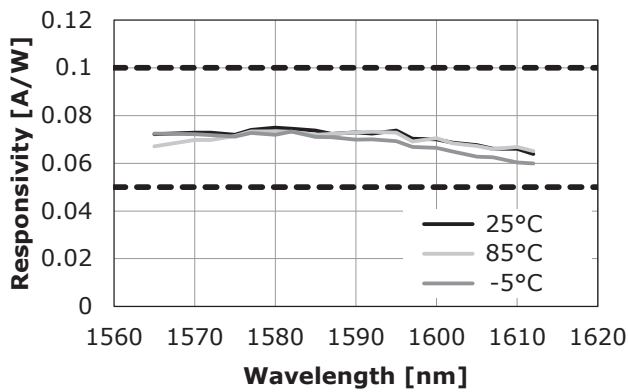
(b) Local light (25°C)

Fig. 5. Wavelength dependence of responsivity

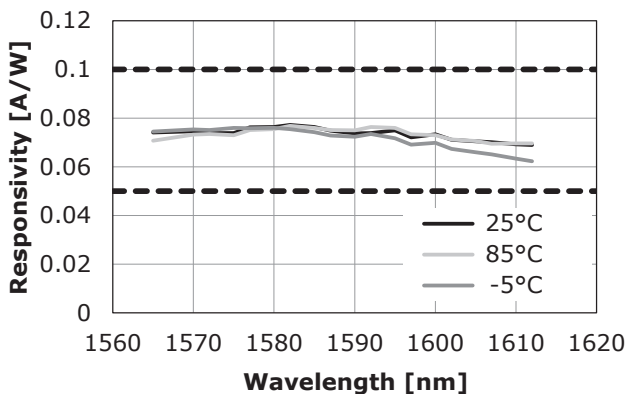
The temperature dependence of responsivity is shown in Fig. 6: (a) indicates the temperature dependence of signal light and (b) indicates the temperature dependence of local light.

For responsivity, the mean value of all the channels was used. We confirmed that the changes in responsivity were very small within the operating temperature range.

To receive signals in the L-band, the multilayer film of the optical parts was optimized for the L-band. In particular, the PBS needs to separate the X- polarization and Y- polarization accurately in the L-band as well.



(a) Signal light



(b) Local light

Fig. 6. Temperature dependence of responsivity

Figure 7 shows the wavelength dependence of the polarization extinction ratio (PER) at 25°C. We confirmed that the ratio was 25 dB or more in all the bands, thus meeting the target characteristics and stably separating the polarized waves in the L-band.

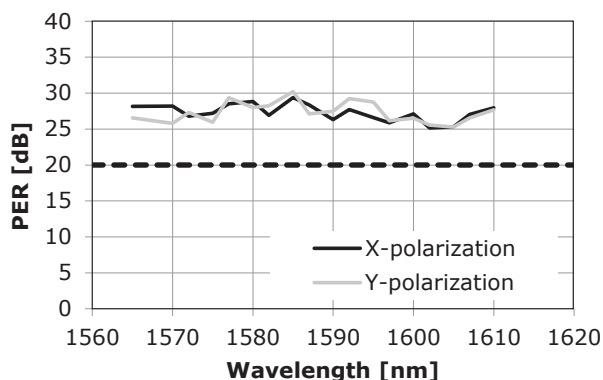


Fig. 7. Wavelength dependence of polarization extinction ratio (25°C)

4-2 Phase characteristics

Figure 8 indicates the wavelength dependence of the I-Q phase error in the X- and Y-polarization.

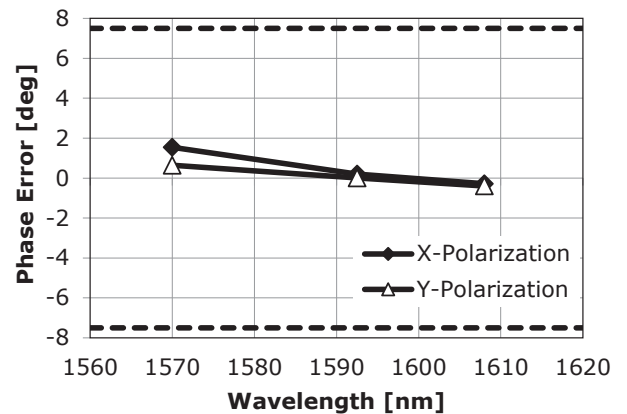


Fig. 8. Wavelength dependence of I-Q phase error (25°C)

The ideal phase angle difference between the I-Q outputs is 90°. The deviation from 90° constitutes a phase error. If the phase error is 0°, the I-Q phase angle difference is 90°, and the constellation*4 is completely symmetrical from the origin. The greater the phase error from 0°, the greater the I-Q imbalance, resulting in a non-square constellation and abnormal demodulation.

We measured the phase between the I-Q outputs for X- and Y-polarization at 25°C to check the deviation from 90°. The deviation was within $\pm 2^\circ$ for both X- and Y-polarization. The characteristics were adequate for proper demodulation.

4-3 High-frequency characteristics

The frequency dependence of the light-electricity conversion gain (normalized for the low-frequency band) is shown in Fig. 9. The measured wavelength was 1590 nm. For the 3 dB band, the difference between the channels was small. The results met the target. The characteristics were adequate for receiving the modulated signals at the symbol rate of 32 GBaud.

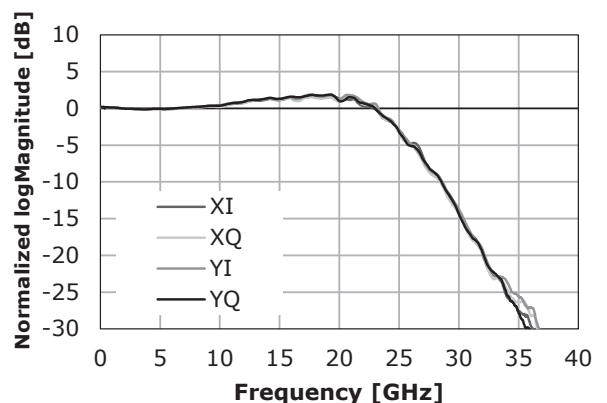
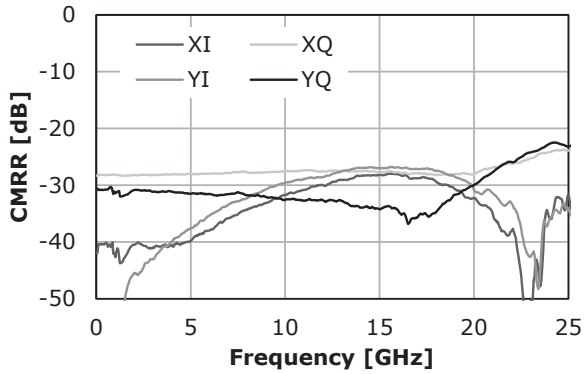
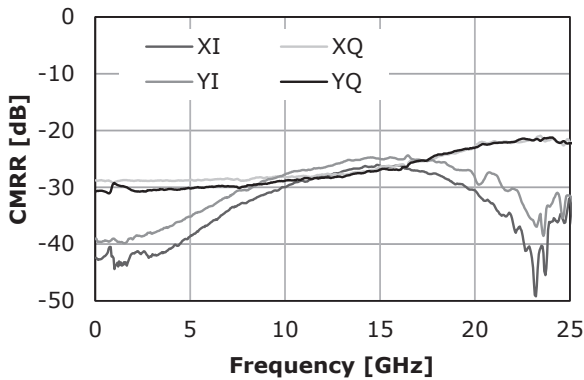


Fig. 9. Frequency dependence

Figure 10 shows the frequency dependence of the common-mode rejection ratio (CMRR), which indicates the influence of the in-phase signals. CMRR was -20 dB or less for both the signal light and local light, showing that the characteristics were favorable and equivalent to those of our coherent receiver for the C-band.



(a) Signal light



(b) Local light

Fig. 10. Common mode rejection ratio

5. Conclusion

We have developed a high-responsivity and wide-band coherent receiver that can function in the L-band. It can be installed in CFP2-ACO.

Responsivity of 0.06 A/W or more was achieved in the wavelength range between 1565 nm and 1612 nm by optimizing the 90° hybrid integrated photodetectors for the L-band. The characteristics were confirmed to be equivalent to those of our coherent receiver for the C-band.

Technical Terms

- *1 Dual-polarization quadrature phase shift keying (DP-QPSK): Two-bit data can be allocated to horizontally and vertically polarized waves in four phases at intervals of 90° . The polarized waves can be transmitted at the same time, enabling transmission of four bits of information in total.
- *2 Optical internetworking forum (OIF): An industry group of optical network technologies that works on standardization. It compiles the results of its reviews as Implementation Agreements (IAs) (i.e., standardization documents).
- *3 Multi mode interference (MMI): A waveguide technology that achieves an $N \times N$ combination/separation waveguide, among others, by utilizing the multimode light interference in a waveguide.
- *4 Constellation: A diagram that presents the amplitude and phase information on a two-dimensional complex plane. In-phase components are plotted on the horizontal axis and orthogonal components on the vertical axis.

References

- (1) M. Takechi et al., "Compact Optical Receivers for Coherent Optical Communication," SEI Technical Review, No. 85 (Oct 2017)
- (2) "Implementation Agreement for Micro Intradyme Coherent Receivers" IA # OIF-DPC-MRX-02.0 (June 21, 2017) <https://www.oiforum.com/wp-content/.../OIF-DPC-MRX-02.0.pdf>
- (3) N. Inoue et al., "InP-based Photodetector Monolithically Integrated with 90° Hybrid for 100 Gbit/s Compact Coherent Receivers," SEI Technical Review, No. 79 (Oct 2014)
- (4) T. Okimoto et al., "InP-based Waveguide Photodetector Monolithically Integrated with 90° Hybrid Having High-responsivity Characteristics over the L-band Wavelength Range," The 2017 IEICE Electronics Society(C-4-11)

Contributors The lead author is indicated by an asterisk (*).

M. GOTOH*

• Sumitomo Electric Device Innovations, Inc.



K. SAKURAI

• Sumitomo Electric Device Innovations, Inc.



M. KUROKAWA

• Assistant Manager, Transmission Devices Laboratory



K. ASHIZAWA

• Manager, Sumitomo Electric Device Innovations, Inc.



Y. YONEDA

• Senior Manager, Sumitomo Electric Device Innovations, Inc.



Y. FUJIMURA

• Group Manager, Transmission Devices Laboratory

